Stereochemical Assignment of Strigolactone Analogues Confirms their Selective Biological Activity

Emma Artuso,[†] Elena Ghibaudi,[†] Beatrice Lace,[†] Domenica Marabello,[†] Daniele Vinciguerra,[†] Chiara Lombardi,[†] Hinanit Koltai,[‡] Yoram Kapulnik,[‡] Mara Novero,[§] Ernesto G. Occhiato,[⊥] Dina Scarpi,[⊥] Stefano Parisotto,[†] Annamaria Deagostino,[†] Paolo Venturello,[†] Einav Mayzlish-Gati[‡] Ariel Bier[‡] and Cristina Prandi[†,]*

[†]Department of Chemistry, University of Turin, via P. Giuria 7 10125 Turin, Italy

[§]DBIOS, University of Turin, viale Mattioli 25, 10125 Turin, Italy.

[⊥]Department of Chemistry "Ugo Schiff", University of Florence, via della Lastruccia 13, 50019 Sesto Fiorentino, Italy

[‡]ARO Volcani Center Bet Degan Israel.

ABSTRACT. Strigolactones (SLs) are new plant hormones with various developmental functions. They are also soil chemical signals required for establishing beneficial mycorrhizal plant/fungus symbiosis. In addition, SLs play an essential role in inducing seed germination in root-parasitic weeds that are one of the seven most serious biological threats to food security. There are around 20 natural SLs that are produced by plants in very low quantity, therefore, most of our knowledge about SLs signal transduction and associated molecular events is mainly based on the application of synthetic analogues. Stereochemistry plays a crucial role in Strigolactones Structure-activity relationship as compounds with unnatural configuration at the D-ring may induce biological effects unrelated to Strigolactones. We have synthesized a series of Strigolactones analogues, whose absolute configuration has been elucidated and put in relation with their biological activity, thus confirming the high specificity of the response. Analogs bearing the R-configured butenolide showed enhanced biological activity highlighting the importance of this stereochemical motif.

Strigolactones (SLs) are a new class of plant hormones whose potential in agriculture applications has been fueling intense research, both applied and pure.[1] They have recently been assessed as a new class of plant hormones having effects on shoot branching[2], root development,[3] photomorphogenesis,[4] besides acting as signaling molecules in the rhizosphere where they induce hyphal branching in arbuscular mycorrhizal fungi (AMF)[5] and seed germination in parasitic plants.[6] Natural SLs all share the same basic framework which consists of a tricyclic nucleus ABC connected with a butenolide (D-ring) by means of an enol ether bridge (Chart 1),[1b] therefore they can be classified as Michael acceptors. More than 20 natural SLs have been identified[1a,7] while it is likely that others will be found in the near future. This leads to questions as to why plants produce blend of SLs and whether quantitative and qualitative differences in SLs production and/or exudation are important in host recognition.[8] More recently still, SLs and analogues have even been shown to act as promising anticancer agents.[9,10] Strigolactones are very active molecules and indeed occur in very low abundances in root exudates, which is why assessments of their biological activity and unambiguous configurational assignments are often hampered.[1a] The structural characterization of natural SLs and extensive structure-activity studies (SAR) have revealed that the bioactiphore resides in the CD (Chart 1) part of the molecule. This has enabled the design and synthesis of SL analogues that show much simpler structures than natural SL but still retain their bioactivity.[11]

Most natural SLs show absolute *R* stereochemistry at the 2' position while the correct stereochemistry of (-)-orobanchol has very recently been unequivocally confirmed.[12] It is now generally accepted that SLs can be stereochemically grouped into two families (Chart 1), one in which the stereochemistry of the BCD part is the same as (+)-strigol (**1**) and the other in which the stereochemistry of the BCD part is the same as (-)-orobanchol (**3**).[13]

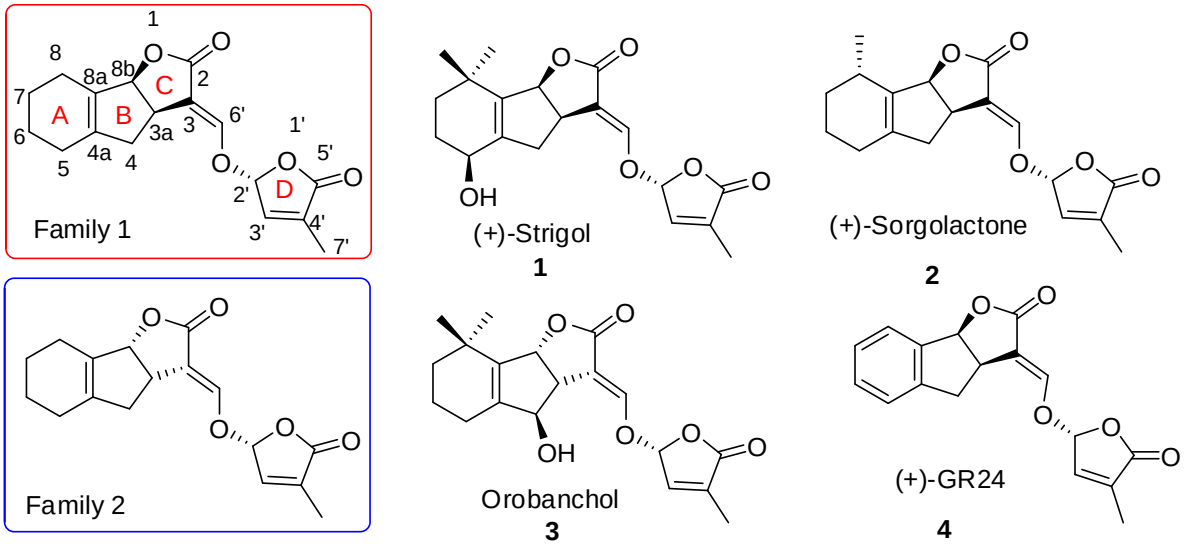

Chart 1. General structure of Strigolactones, Stereochemistry of some natural SLs and of the synthetic analogue (+)-GR24

An analysis of mutants that are insensitive to pharmacological applications of SLs has led to the identification of DAD2 in petunia as the putative receptor that is able to hydrolyze SLs.[14] DAD2, AtD14 (*Arabidopsis thaliana*) and D14 (*Oryza sativa*) have been assessed by X-ray analysis and found to belong to the α,β-hydrolases family.[15] In *Arabidopsis thaliana*, α,β-hydrolases KAI2 and AtD14 are responsible for responses to karrikins,[16] chemical compounds found in plant-derived smoke,[17] and SLs respectively. Although KAI2 mediates responses to KARs and to some SLs analogues, AtD14 mediates SLs response only. It was recently demonstrated that AtD14 and KAI2 exhibit selectivity to the strigolactone D-ring configurations 2'*R* or 2'*S*, respectively.[18] Structure Activity Relationship studies on shoot branching inhibition in rice and Arabidopsis have recently demonstrated that the (R) configuration at C-2' has significant influence on the hormonal activity.[19]

An assessment of the stereochemistry of SLs and analogues is therefore mandatory to avoid the activation of responses that are not related to SLs and therefore the misinterpretation of our results. Furthermore, the use of pure stereoisomers can furnish valuable information on the structural requirements for distinct perception systems in plants, parasitic weeds and arbuscular mycorrhizal fungi.

Difficulties in synthesizing natural SLs, caused by the long multistep syntheses, and their low availability from natural sources have prompted chemists to develop synthetic analogues that are easily accessible in sizeable quantities, stable and whose activity could be related to that of natural SLs. One added advantage of this approach is the ability to obtain more information about the structural requirements for the activation of specific perception systems and specificity of the target functions.

Our contribution to the field has been the development of a family of indolyl derived analogues named EGOs.[20]

The synthetic procedure is feasible as it starts from cheap reagents and multigram preparations are easily accomplished. The analogues were designed with the specific aim of reducing stereochemical complexity, and in fact the only stereocenter retained is the 2' position. Compounds that are obtained as racemic mixtures are easily separated by chiral semipreparative HPLC (see SI). Several biological assays have been carried using EGO analogues[21] on various target systems in the past and some new ones are herein presented, yet we have not elucidated the absolute configuration of pure enantiomers, until now.

In this paper we report the assignment of the absolute stereochemistry of the parent EGO10 compounds (**5, 6** Chart 2) by X-ray analysis and circular dichroism and the configuration of the

other members of the family, by comparing CD spectra. Once the absolute configuration of the pure enantiomers is established, we then correlate some past, and other unpublished results with the biological effects induced by the EGO analogues, thus shedding light on the importance of stereochemistry in SLs response. A EGO10 derivative (MEB55), which is active as an anticancer agent, and some fluorescent tagged analogues (EGOBP and BPGR24), which are used for bio imaging applications, are included among the analogues taken into consideration..

RESULTS AND DISCUSSION

Our interest in developing new synthetic SL analogues is manifested in two principles aims: a) to deepen the structure-activity relationship in varying systems for each of the different roles ascribed to SLs and b) to develop active fluorescent SL active analogues that are suitable for bioimaging studies and *in vivo* detection to map Strigolactones distribution in plants and fungi. We have recently reported the synthesis of a new class of Strigolactone analogues that show interesting luminescent properties.[22] We have also developed a new class of indolyl derived compounds named EGO which can be functionalized with different substituents on the A ring.[21b,23] Furthermore in view of the use of SL analogues as fluorescent probes in the *in vivo* mapping of the dynamic processes in which SLs are involved, we have designed a new generation of fluorescent analogues whose properties are suitable for confocal microscopy investigations using the well-known fluorescent BODIPY based probes.[24]

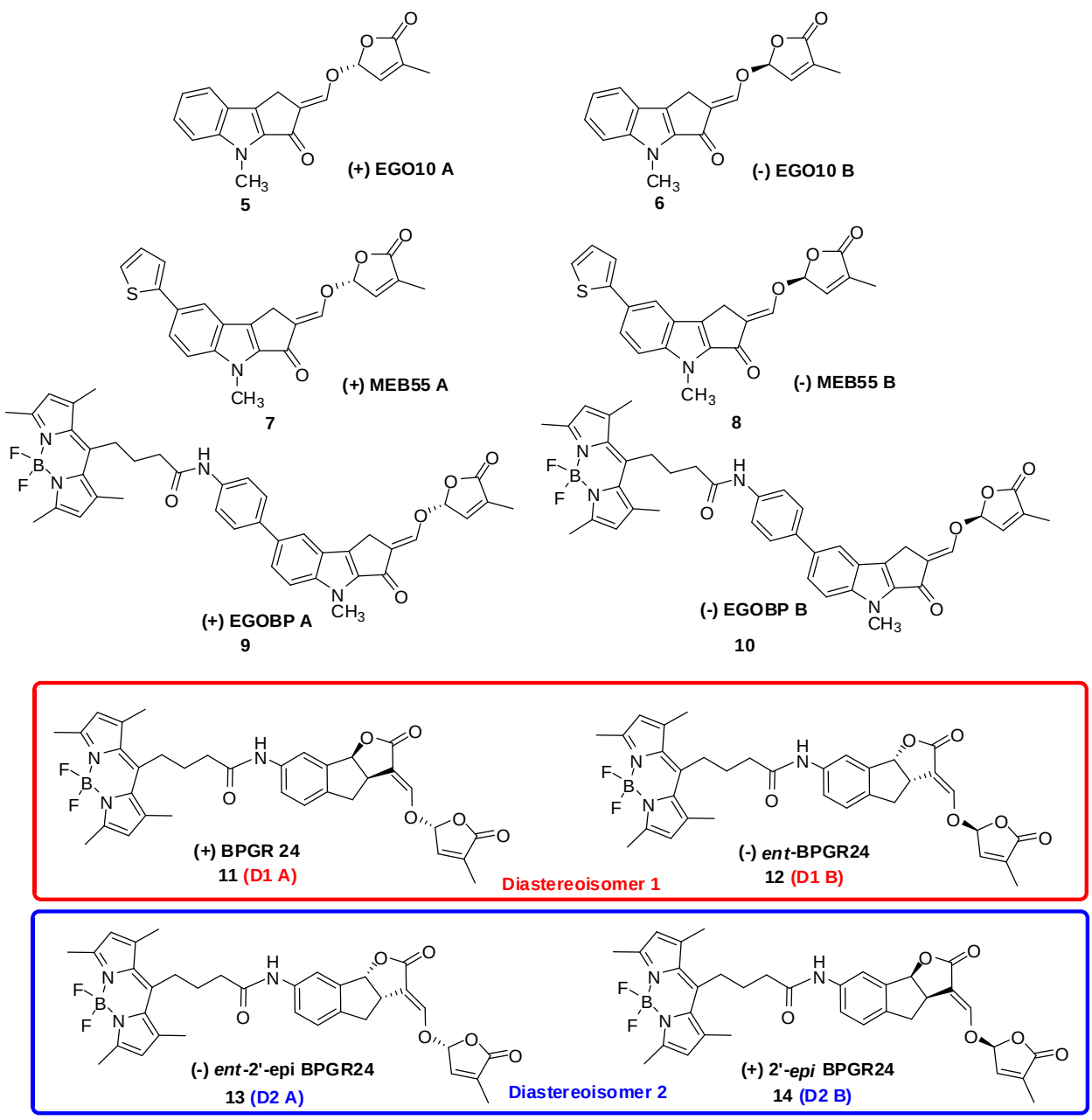

Chart 2. Series of SLs analogues separated as pure enantiomers

EGO10 (**5, 6**) and MEB55 (**7, 8**) were synthesized as previously described.[21b,23]EGOBP A (**9**) and EGOBP B (**10**) were synthesized and used for *in vivo* visualization.[22] In addition, we decided to use SL analogue GR24 (**4**) as our core structure due to its widespread use as standard for

biological assays. The fluorophore BODIPY can be linked to GR24. To this purpose we synthesized amino-GR24 (**19**, Scheme 1) from nitro- derivative **15**, but with a slight modification to the reported procedure.[25]

Compound **4** was obtained as a mixture of stereoisomers, more specifically as two racemic diastereomers **18** which were separated by column chromatography**.** From this point onwards, the reactions were carried out on both the diastereomers separately.

Scheme 1. Synthetic procedure to BPGR24 as a mixture of stereoisomers[a]

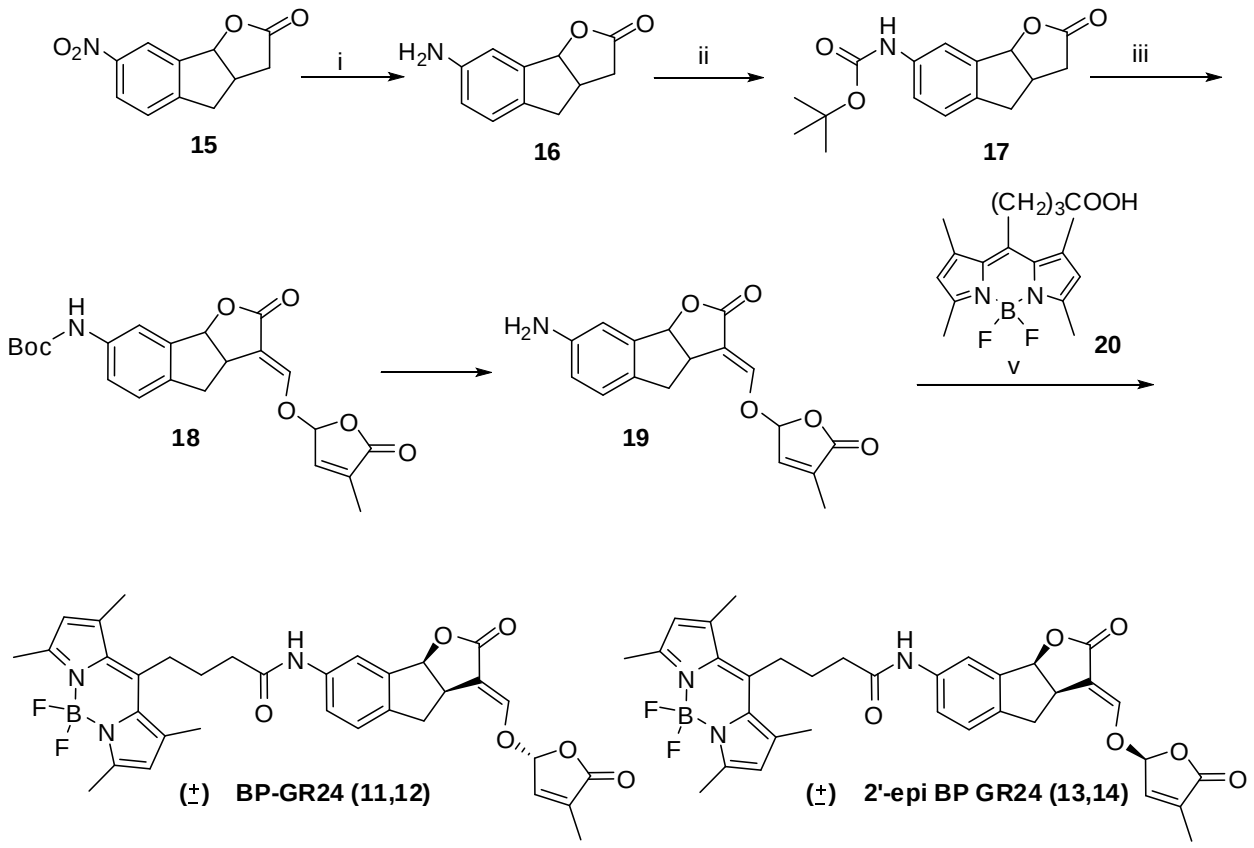

[a]Reagents and conditions: (i) ZnCaCl2, EtOH-H_2O, reflux, 2 hs (80%); *t*-Boc_2O, DMAP, THF, reflux, 18 hs (80%); HCOOEt, *t*-Boc_2O, DME, rt, 2 hs then 5-bromo-3-methylfuran-2(5H)-one, rt,.18 hs (62%); (iv) TFA, DCM, rt, 2hs (93%) then 6, CDMT, NMM, DCM, rt, 18 hs (78%).

After the introduction of the D-ring, compound **18** was deprotected and coupled with the corresponding BODIPY fragment **20** according to the Kaminski procedure and obtained with a 78% yield.[26] The racemic mixtures were then separated via chiral HPLC (see SI) and the four stereoisomers BP GR24 (**11**), *ent* BPGR24 (**12**), 2'-*epi* BP GR24 (**13**) and *ent* 2'-*epi* BP GR24 (**14**) were fully characterized. The absolute configuration was determined on the base of CD spectra as described in the next section, and *via* a comparison of chromatographic behavior with parent GR24 standards.

X Ray analysis. Crystals of EGO10A (**5**) that were suitable for X-ray diffraction analysis were obtained via a slow evaporation of a methanol solution. Seeing as the molecule is only composed of light atoms, X-ray data were collected using Cu-Kα radiation (λ=1.5418 Å), which furnishes a more accurate determination of absolute configuration even when heavy atoms are not present in the molecule. The ORTEP plot of the molecule is reported in Figure 1.

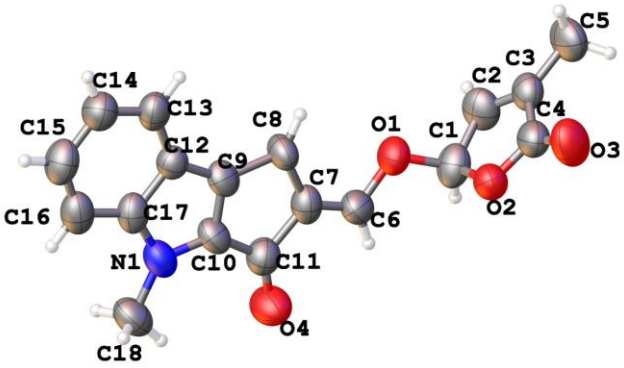

Figure 1. ORTEP plot of compound EGO10A (**5**) with atom labeling. Thermal ellipsoids of non-hydrogen atoms are represented at 50% probability.

Although the diffraction capability of the crystal was low, the data collected were sufficient to clearly determine the absolute configuration, via the Parsons method.[27] As shown in **Figure 1** the resulting absolute configuration of compound EGO10A is *R* at the C-1 (C-2') stereocenter.[28]

CD measurements. The CD spectra of submillimolar solutions of each EGO10 (**5, 6**) and EGOBP (**9, 10**) stereoisomer were recorded in acetonitrile, in order to collect evidence concurring to the determination of the absolute configuration of the C2'stereocenter.

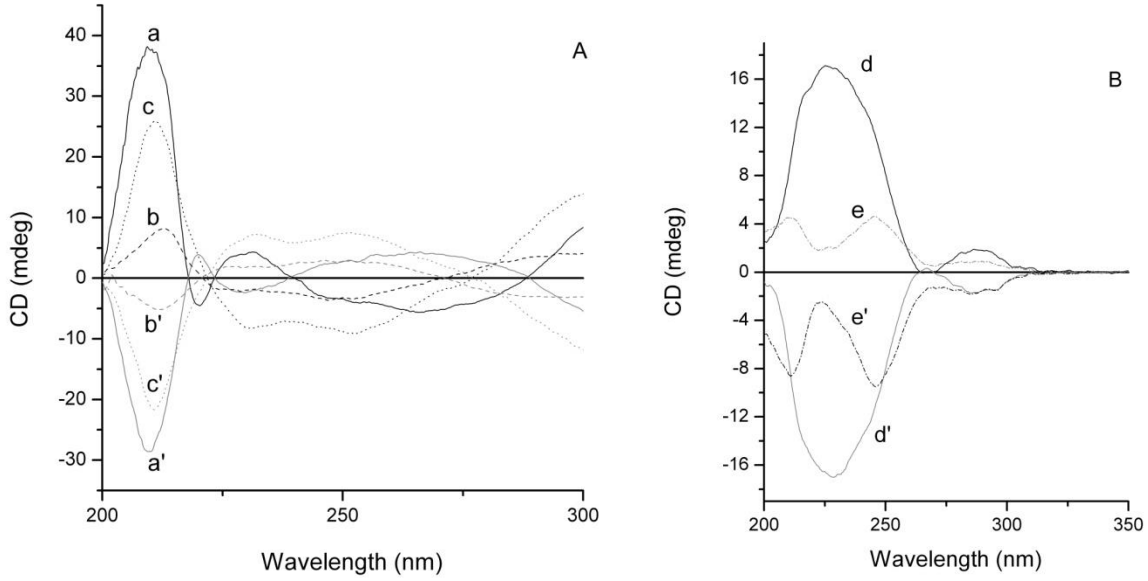

Figure 2 - Panel A: CD spectra of EGO10 A (**5**, a) and B (a'), EGOBP A (**6**, b) and B (7, b'), MEB 55 A (**6**, c) and B (**7**, c'); Panel B: CD spectra of BPGR24 (**11**, d) ent-BPGR24 (**12**, d'), ent-2'-epi-BPGR24 (**14**, e) and 2'-epi-BPGR24 (**13**, e'). *R* stereoisomers at C-2' are outlined in black; *S* stereoisomers at C-2' are outlined in dark grey. All stereoisomers were dissolved in acetonitrile at submillimolar concentration.

Figure 2 (**panel A**) reports the CD spectra of enantiomers A and B of EGO10, EGOBP and MEB55 in the 200-300 nm spectral region. All these compounds contain a single stereocenter (C-2'). The labels A and B were initially assigned according to HPLC behavior of the enantiomers: the A species eluted before the B species in our experimental conditions (see SI). The spectral patterns associated with the three 'stereoisomers A' share similar features, and the same is true for the 'stereoisomers B' set. The full CD spectra of these compounds in the 200-450 nm range are reported in the SI (Figure 1S). The stereochemical assignments of SLs stereocenters by CD spectroscopy generally relies on the empirical rule proposed by Frischmuth *et al.*[29] According to this rule, compounds that exhibit a negative CD around 270 nm have a C-2'*R* configuration, whereas a positive CD band is typical of C-2'*S* stereocenters. The rule is grounded on two basic assumptions: i) an absence of electronic interactions between chromophoric systems C and D; ii) the conformational identity of epimers C-2'. According to these assumptions, rings C and D provide independent contributions to the CD spectrum and the spectral region around 270 nm is mainly related to electronic transitions that involve the ring D chromophore. Despite the clearly approximate character of such assumptions, the rule has proven to be effective for a number of strigolactone stereoisomers.[30] As far as EGO10, EGOBP and MEB55 compounds are concerned, stereoisomers A exhibit a negative CD band around 270 nm; hence, according to Frischmuth's rule, the absolute configuration of the C-2' center is *R* in all three compounds, whereas stereoisomers B exhibit a C-2'S arrangement. This assignment is supported and confirmed by a number of consistent pieces of evidence. In fact, the X-ray structure of EGO10 A (**5**) unambiguously shows a C-2'*R* configuration. In addition, the three stereoisomers that belong to set A are chemically correlated, in that they are obtained via a synthetic procedure that cannot perturb stereocenter C-2'. The same is true for set B. Hence each

set must share the same absolute configuration at C-2'. A further supporting evidence is the fact that the chromatographic behavior of stereoisomers A stereoisomers A vs. B towards chiral phases is homogeneous within sets. This argues in favor of the same absolute C-2' stereocenter configuration in each set of molecules. All the evidence collected on EGO10, EGOBP and MEB55 are consistent with the assignment of the C-2'*R* configuration to set A and the C-2'*S* to set B. Figure 2 (**panel B**) reports the CD spectra of the 4 diastereoisomers BPGR24 (**11**), *ent*-BPGR24 (**12**), 2'-*epi*-BPGR24 (**14**) and *ent*-2'-*epi*-GR24 (**13**, Chart 2). These compounds exhibit peculiar CD spectral patterns, unlike the previous sets of molecules as well as other known strigolactones. In particular, no CD bands' sign inversion is observed in the 200-350 nm range and Frischmuth's rule is no longer applicable. This is probably related to the disappearance of the premises upon which the rule was grounded: either conformational issues influence the spectral pattern or the claimed electronic independence of ring C and D can no longer be assumed. A completely unambiguous assignment of the absolute configuration in the presence of conformational or electronic factors might require a complex approach, based on the combination of ECD, VCD and theoretical calculation.[31] Nevertheless, the combination of several distinct experimental findings (X-ray structure, ECD data, chemical correlation and chromatographic behavior) provides sufficient evidence for the configurational assignment by analogy. In fact, as these compounds are GR24 derivatives, CD spectra may be analyzed by comparison with the well-known CD patterns of GR24 and its diastereoisomers [32](see Figure 2S, SI) which do not follow Frischmuth's rule either. (+) GR24 (**4**) has been definitely shown by Scaffidi et al. to display a C-2'*R* configuration and its CD spectrum exhibits a positive band in the 210-260 nm range. Both BPGR24 (**11**) and *ent*-2'-*epi*-BPGR24 (**12**) show positive absorptions in the very same spectral region, which suggests an analogue C-2'*R* configuration for

both of them. The distinct features of the CD patterns of diastereoisomers BPGR24 (**11**) and *ent*-2'-*epi*-BPGR24 (**12**) are certainly related to differences in the electronic levels energies: *ent*-2'-*epi*-BPGR24 (**13**) exhibits three resolved bands while BPGR24 (**11**) apparently shows only two. However, the band at ~230 nm is clearly not a pure Gaussian curve, which means that it is the convolution of more than one contribution. Hence, the CD spectra of BPGR24 and *ent*-2'-*epi*-BPGR24 are overall consistent. Further arguments in support of the C-2'R assignment for BPGR24 and *ent*-2'-*epi*-BPGR24 are the chemical correlation between these two stereoisomers and (+) GR24 as well as analogies in the chromatographic behavior of the species. In conclusion, CD data collected on the EGO and BPGR24 series of strigolactones clearly show that EGO derivatives fulfill Frischmuth's rule, whereas BPGR24 derivatives do not. Experimental evidence converges towards the assignment of *R* configuration for C-2' stereocenter of EGO10 A (**5**), EGO-BP A (**9**), MEB55 A (**7**), BPGR24 (**11**) and *ent*-2'-*epi*-BPGR24 (**13**).

Biological activity. The simplest molecules that were separated as pure enantiomers were EGO10 A (**5**) and EGO10 B (**6**) whose absolute configuration corresponds to *R* for EGO10 A and *S* for EGO10 B, as demonstrated by X-ray analysis and circular dichroism.

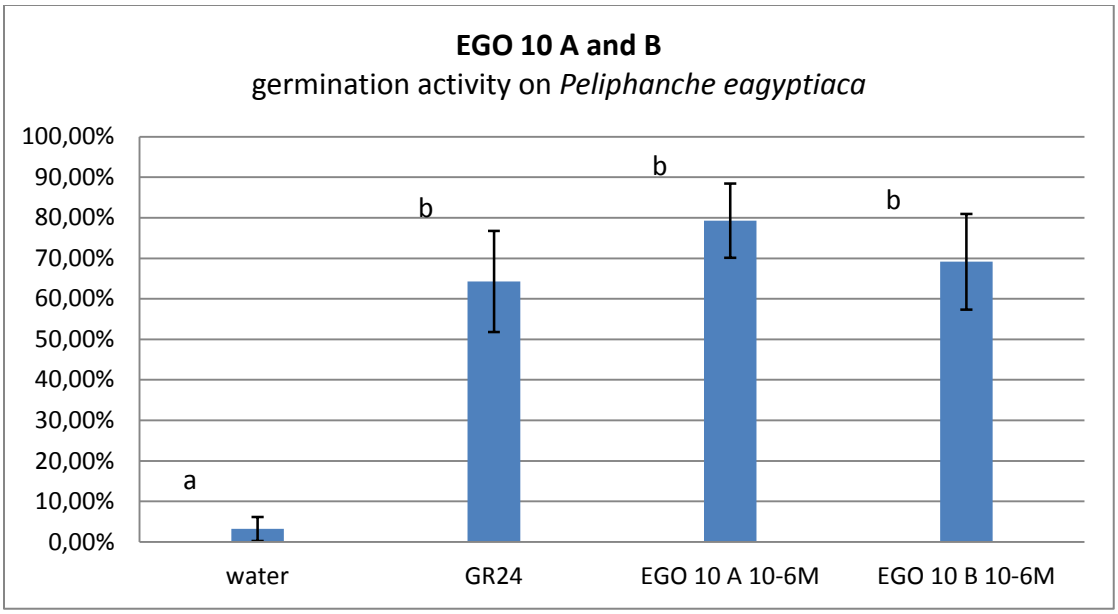

Figure 3. Bar graph representation of germinated seeds percentages (Y axis) of *Phelipanche aegyptiaca* after exposure to pure enantiomers of EGO10 A and B.

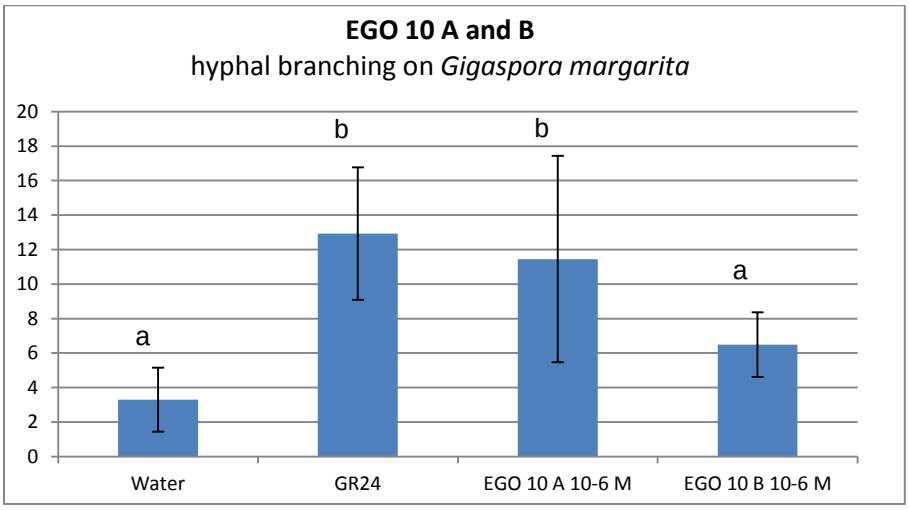

Figure 4. Bar graph representation of hyphal branching number per hyphal apex of *Gigaspora margarita* after exposure to the two pure enantiomers of EGO10 A and EGO10 B.

Figures 3 and 4 clearly show that enantiomers EGO10 A and EGO10 B exhibit significantly different activity in the hyphal branching test, EGO10 A (*R*) is the most active here, while

conversely, the activity of these enantiomers on *Peliphanche aegyptiaca* seeds does not show any statistical difference.

This result is consistent with the recently reported literature data according which the non-natural enantiomer of SLs could activate biological responses through perception systems unrelated to SLs.[32]

Root hair elongation. The hormonal activity of the enantiomers of EGO10 on root hair elongation has also been evaluated on *Arabidopsis thaliana*, using a well-established protocol.[33] Racemic EGO10' s strong positive effect on RH elongation has already been demonstrated.[34]

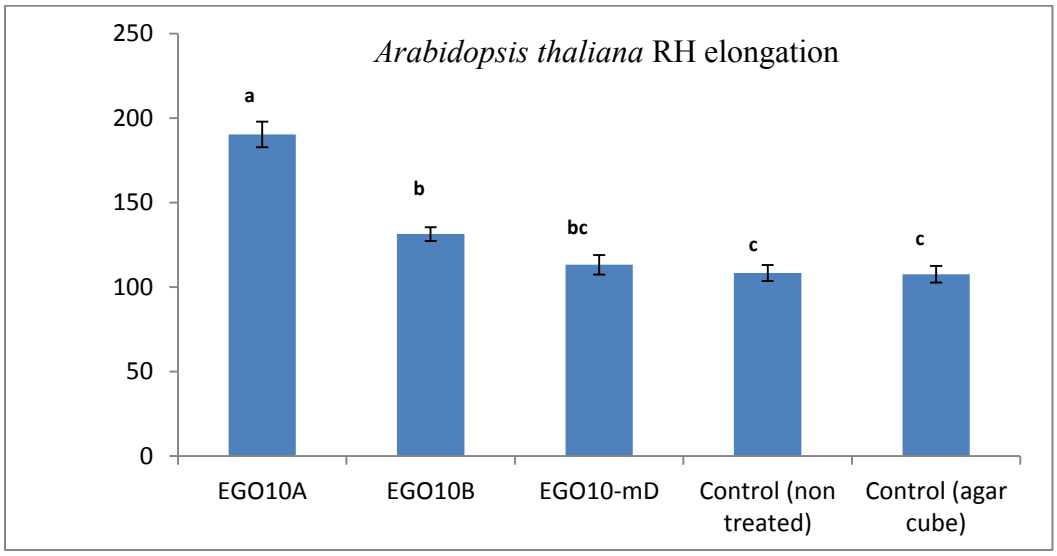

Figure 5. Root hair length (µm) in root segments of *Arabidopsis thaliana* after exposure to EGO10A, EGO10B, EGO10-mD at 0.1 µM concentration.

As shown in the bar graph in Figure 5, the effect of EGO10A (*R)* is statistically larger than that of its enantiomer EGO10B (*S*). In addition the effect of EGO10 without the D-ring (EGO10-mD) was considered in order to demonstrate the role of the enol ether bridge and the D-ring in inducing biological effects. In fact, EGO10-mD was as ineffective as EGO10 B.

MEB55. Thiophene derivatives were synthesized according to known procedure and separated into pure enantiomers (see SI). The activity of racemic mixtures of MEB55 had already been tested on *Peliphanche aegyptiaca* seeds and good activity was reported.[23]

We then measured the activity of enantiomers at the same concentration at which the racemic mixture proved to be most active. As shown in **Figure 6** the two enantiomers behave differently, MEB55 A (**7**, 2'*R*) is much more active than both of MEB55 B (**8**, 2'*S*) and racemic GR24 which was used as a standard.

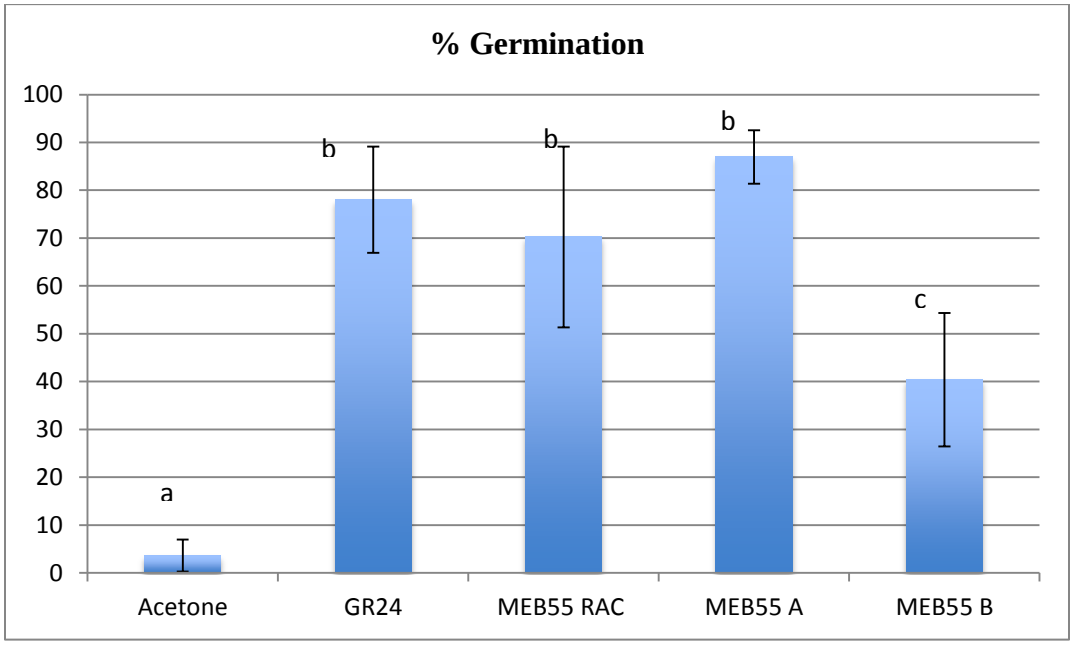

Figure 6. Bar graph representation of percentages of germinated (Y axis) of *Peliphanche aegyptiaca* seeds after exposure to pure enantiomers of **MEB55 A** (**7**) **and B** (**8**) at 0.1 µM concentration**.**

We recently reported the antiproliferative activity of some SLs analogues.[9] After an initial screening of EGO10 derivatives that had seen various substitutions on the A ring, those with a thienyl (MEB55) and dioxathienyl substituent at the 7 position were found to be the most potent

and promising candidates for anticancer therapy thanks to their ability to specifically induce cell cycle arrest, cellular stress and apoptosis in cancer line cells with minimal effects on normal cells growth and survival. Two different cell lines have been tested for their response to enantiopure SLs analogues. The first line BJ is a normal cell line established from human neonate fibroblasts (skin, foreskin), the second MDA-MB-231, from human breast cancer cells (epithelial, adenocharcinoma disease).[9] Enantiomer activity on cell lines was quantified as the effect on cell viability, using XTT (see SI). As shown in Figure 7, the normal cell line BJ is insensitive to SL analogues application while the viability of the tumor cell line MDA-MB-231 is affected by SLs. In particular one of the two enantiomers MEB55 A (**7**), which corresponds to the R configuration at C-2' (red bar, Figure 7) was found to be much more active than the S stereoisomer. The racemic mixture of the two enantiomers (purple bar, Figure 7) and the equimolar mixture of *R* and *S* enantiomers, created to have an additional control (light blue), show activity which is similar to the most active *R* enantiomer indicating that the *S* enantiomer does not possess antagonist activity.

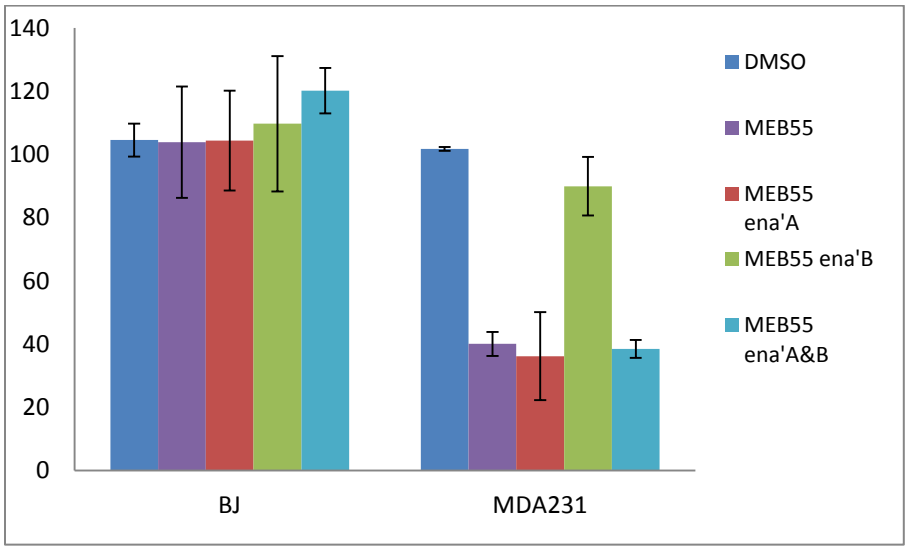

Figure 7. Bar graph representation of cell viability test on cell lines BJ and MDA-MB-231 in the presence of MEB55. 2500 were seeded per line. They were treated with a 7.5 μM solution of compound MEB55 after one day. XTT measurements for the determination of cell viability were carried out after 48h-after exposure to compound MEB55.

EGO BP. Spatial hormones distribution is actively regulated by plants at multiple levels, such as biosynthesis, catabolism and transport to allow specific function to occur. The level of SLs secretion is also likely to be properly controlled. The *Petunia hybrid* ABC transporter PDR1 has recently been isolated.[35] However only little is known about the dynamic distribution of SLs, their precursors and their derivatives in *Arabidopsis* in particular.[36] As part of our work on the synthesis of fluorescent tagged SLs analogues to map the distribution of SLs in plants we have synthesized EGO10 derivatives by linking the EGO10 core to a fluorescent BODIPY based probe, through a 3 C linker (Chart 2, EGO BP A **9** and EGO BP B **10**). The activity of racemic EGO BP had previously been tested on *Peliphanche aegyptiaca* seeds and found to be a little lower than rac-GR24,[20] as expected. Racemic EGO BP was resolved in the two enantiomers EGO BP A (**7**) and EGO BP B (8) whose absolute configuration was unambiguously assessed according to CD spectra and chiral HPLC behavior (SI); EGOBP A being the *R* enantiomer and EGOBP B the *S*. Fluorescence emission measurements of Arabidopsis seedlings treated with fluorescent SLs showed a higher accumulation of EGOBP A than EGOBP B in the root. Moreover EGOBP A was the most active root hair elongation analogue. Controls were performed using fluorophore BODIPY(naked-BP) alone which led to non-specific tissue distribution and with EGOBP which was missing the D-ring and the enol ether connecting bridge which also lead to non specific distribution. Given these preliminary but clear-cut results

EGOBP A was then chosen as the lead candidate with which to follow the distribution and transport of SLs in *Arabidopsis*.[37]

BPGR24. Because of its widespread use and the huge body of data available on its biological activity in different organisms we decided to functionalize the universal standard GR24 with the same fluorescent probes BODIPY and check for the bioactivity of the four stereoisomers (Chart 2).

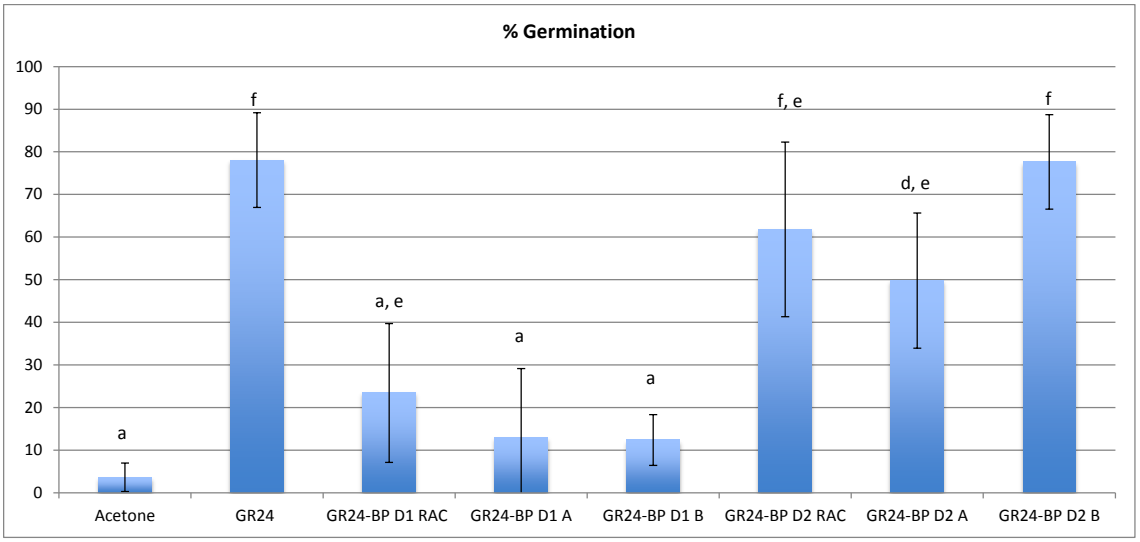

Figure 8. Bar graph representation of percentages of germinated seeds (Y axis) of *Peliphanche aegyptiaca* after exposure to pure enantiomers of the GR24 BP serie at 0.1 µM concentration

The germination stimulatory activity of all four GR24 BP stereoisomers was measured towards *Peliphanche aegyptiaca* seeds. The results shown in Figure 8 surprisingly revealed that the D1 diastereoisomer is completely inactive and statistically comparable to the negative control acetone, whether used as a racemic mixture or a pure enantiomer. It is worthy emphasizing that GR24, whether used as a racemic or a pure enantiomer. (*rac*-GR24 vs. (+) GR24 and (-) *ent* GR24, see SI) show the predicted germination activity. Besides, the D2 diasteroisomers both as

racemate and as pure enantiomer (2'-epi BPGR24 **14** and *ent*-2'-epi GR24BP **13**) show germination activity that is comparable to rac-GR24. This was then chosen as the lead candidate for bioimaging studies into SLs transport and distribution in living organisms.[38]

In this study**,** we were able to elucidate the absolute configuration of a series of enantiomerically pure SL analogues by means of X-ray analyses of one of the compounds and by the comparative analysis of the CD spectra of all family members. This was based on the fine correlations found within the whole family of compounds and with the literature data.

Recent findings demonstrate that the stereochemistry at the 2' position (D-ring) plays crucial roles in the activation of specific response related to SLs.[32] As stereochemistry has been proven to be a significant determinant of SL activity, we examined multiple physiological responses in various organisms in order to correlate the absolute configuration to activity. We decided on using parasitic seeds germination (*Peliphanche aegyptiaca*), hyphal branching (*Gigaspora margarita*), root elongation (*Arabidopsis thaliana*) and cell cycle arrest of cancer and non-cancer cell lines as the biological targets. Wherever selectivity towards one of the two enantiomers is observed, the enantiomer with *R* configuration at the C-2' is the most active. In the Orobanchaceae, *S. hermontica* seeds are reported to respond to all stereoisomers of GR24[1a] and deoxystrigol[30] with a slight preference for isomers with the same configuration as natural strigol. The four stereoisomers of deoxystrigol have recently been tested on *Orobanche minor* and it was found that the stereoisomer with the same configuration as orobanchol was the most active while its enantiomer the least active so.[32] However, 2'-*epi* BPGR24 (**14**, 2' *S*) is the most active fluorescent derivative of GR24.

In summary, the present work sees an elucidation of the absolute configurations of some of the most potent SL analogues that have been designed for specific purposes. We have also discussed the correlation between stereochemistry and biological response.

EXPERIMENTAL SECTION

General experimental procedures

^{1}H NMR and ^{13}C NMR spectra were recorded on a Bruker Avance-200. ^{1}H NMR spectra were recorded at 200 MHz, ^{13}C NMR and DEPT spectra at 50 MHz. ESI-MS spectra were recorded using a LCQ Deca XP plus spectrometer (Thermo) spectrometer with an electrospray interface and ion trap as a mass analyzer; sheath gas flow rate was set at 25 (arbitrary unit), auxiliary gas flow rate at 5 (arbitrary unit), spray voltage at 3.25 (KV), capillary temperature at 270 °C, capillary voltage at −7 (V), and tube lens offset at −60.00 (V). Nitrogen was used as a sheath and auxiliary gas. High-resolution data were recorded on an LTQ Orbitrap Hybrid Mass Spectrometer. MS spectra were recorded at an ionizing voltage of 70 eV.

Chromatographic separations were carried out on silica gel (Merck Grade 7734, pore size 60 Å, 70-230 mesh); Rf values refer to TLC carried out on 0.25-mm silica gel plates (Merck F254), with the same eluent indicated for the column chromatography.

All the chemicals were purchased from Sigma-Aldrich and were used as received unless stated otherwise. Column chromatography purifications was performed via classical chromatography.

Compounds **15**, **17**, **18** and **19** were synthesized as previously reported.[25]

The glassware used for classical syntheses was heated overnight in an oven at 150°C and assembled in the oven, then cooled under argon flux before starting the reactions.

A Jasco P-2000 polarimeter was used for the determination of optical rotations.

The enantiomers were separated on either a semi-preparative and an analytical Chiralpak IC column (particle size 5 μm, Daicel, Osaka, Japan). Dimensions: Analytical column 4.6 Φ x 250 mmL; Semiprep. column 10 Φ x 250 mmL.

UV Circular Dichroism measurements were performed on a JASCO J-815 instrument at RT, in quartz cells with 1 mm optical path; scanning speed 100 nm/min, bandwidth 1 nm.

Biological tests. Plant material. Seeds of *Peliphanche aegyptiaca* were collected from field grown tomato in the West Galilli of Israel. The seeds were stored in glass vials in the dark at room temperature until use in germination tests. Preparation of test solutions: the compound to be tested were weighted out very accurately and dissolved in 1 mL of acetone and then diluted with sterile distilled water to reach the desired concentrations. All solutions were prepared just before use. Seeds were surface sterilized and preconditioned according to the experimental procedure indicated in ref. 31. Briefly, seeds were exposed to 50% (v/v) aqueous solutions of commercial bleach for 5 min (2% hypochlorite) and rinsed with sterile distilled water. For preconditioning, seeds were sown on a glass fiber filter paper disc using a sterile toothpick (approximately 20 seeds per disc), the glass fiber discs were placed on 2 filter paper discs, dampened with sterile distilled water and incubated at 25 °C in the dark for 6 days. The preconditioned seeds were then allowed to dry completely in the laminar flow, treated with the strigolactone analogue solutions and germination rate was evaluated under a stereomicroscope 7 days after treatment. At least 100 seeds were analyzed at each concentration, synthetic strigolactone GR24 10^{-7}M was included as positive control while an aqueous solution of 0.1% acetone and sterile distilled water was included as negative control. Seeds were considered to be germinated if the radicle protruded through the seed coat.

Fungal material. Spores of *Gigaspora margarita* Becker and Hall were collected from an previously established trap culture of clover, sterilized with a solution of chloramine T (3% P/V) and streptomycine sulphate (0,03% P/V), rinsed with distilled water and placed in a Petri plate filled with 0.2 % Phytagel gel (Sigma-Aldrich) containing 3 mM $MgSO_4$. The plates were incubated vertically for 5 days at 30 °C in the dark. Paper discs (6 mm diameter), loaded with the strigolactone analogue solution, were positioned on either side of the germinating hyphae tips. The number of newly formed hyphal apex were recorded 24 h after treatment. GR24 10^{-7}M was included as positive control, while an aqueous solution of 0.1% acetone and sterile distilled water was included as negative control.

Cell proliferation assay XTT Cell Proliferation Assay. Cells were seeded into a 96 well plates at 2,500 cells per well in triplicates in normal growing media. On the following day, the media was replaced with phenol red-free DMEM supplemented with 10% FBS (Foetal Bovine Serume) and 5% Penicillin-Streptomycin solution. Cells were incubated over night at 37 °C in a

humidified 5% CO_2-95% air atmosphere, and then were treated as indicated below for 48h. An XTT (2, 3,-bis(2-methoxy-4-nitro-5-sulfophenyl)-5-[(phenylamino)-carbonyl]-2H-tetrazolium inner salt) reduction was used to quantify viability according to manufacturer's instruction (Biological industries, IL). Cells were incubated with XTT reagent for 2 h at 37 °C in a humidified 5% CO2-95% air atmosphere. Absorbance was recorded on a VersaMax ELISA Microplate Reader (Molecular devises, USA) at 450 nm with 650 nm being the reference wavelength. Cell survival was estimated from the equation: % cell survival of control= 100 × (At-Ac)(treatment) / (At-Ac)(control), where At and Ac are the absorbencies (450nm) of the XTT colorimetric reaction in treated and control cultures respectively minus non-specific absorption measured at 650nm. Absorbance of medium alone was also deducted from specific readings. Data points were connected by non-linear regression lines of the sigmoidal dose-response relation in dose response assays.

Synthesis of 7-amino-3,3a,4,8b-tetrahydro-2H-indeno[1,2-b]furan-2-one (16): A solution of **15** (3.12 mmol, 0.684 g) in 4.8 mL of ethanol was added to an aqueous solution of $CaCl_2$ (2.18 mmol, 0.684 gin 3.6 mL of water) in a three-necked round bottom flask. Zn powder of was then added (27.52 mmol, 1.80 gr) and the resulting suspension was heated to reflux temperature (80 °C) and reacted for 2 hours. Upon TLC control (petroleum ether/Ethyl acetate, 1/1, Rf = 0.21), which indicated the total consumption of the starting material, the reaction mixture was filtered on a Büchner and washed with CH_2Cl_2. The organic phases were then washed with brine (1x 25 mL) and water (2x 25 ml), dried on K_2CO_3, filtered and the solvent was stripped off. Compound **2** was obtained as 0.420 g (80% yield) of a whitish solid and did not require further purification. ^{1}H NMR ($CDCl_3$, 200 MHz): δ 2.30 (1H, dd, J = 18 Hz, J = 5.8 Hz, H3a), 2.63-2.86 (2H, m, H3), 3.05-3-51 (2H, m, H4), 3.57 (2H, br, NH_2), 5.73 (1H, d, J = 7.0 Hz, H8b), 6.61 (1H, dd, J = 2.0 Hz , J = 8.0 Hz, H6), 6.71 (1H, d, J = 2.0 Hz, H8), 6.98 (1H, d, J = 8.4 Hz, H5). Spectroscopic data correspond to literature reports.[39]

rac- BPGR24 (and rac 2' epi BPGR24). A solution of **20**[21b] (0.15 mmol, 50 mg) was prepared in 3 mL of DCM in a three rounded bottom flask, 2-chloro-4,6-dimetoxy-1,3,5-triazine (CDMT, 0.18 mmol 32 mg) was then added and the solution was refrigerated to -5°C. *N*-methylmorpholine (NMM) was added and the mixture reacted for 2 hours. When the TLC control (petroleum ether/ ethyl acetate 2/3) confirmed the formation of the activated BODIPY complex (approximately 2hs) rac amino GR24 **19** (or rac 2'-epi GR24, 0.150 mmol 47 mg) was added via cannula. The mixture was reacted at room temperature overnight. A 10% solution of citric acid was added and the aqueous phases extracted with DCM (10 mL x3). The organic phases were then dried on Na_2SO_4, and the solvent stripped off under reduced pressure. The crude was purified by flash chromatography with hexane/ethyl acetate 2/3 (Rf 0.20 green fluorescence). And give 74 mg (78% yield) of an orange solid of BPGR24/ent-BPGR24.
Separation on chiral HPLC gives pure enantiomers.

BPGR24 (11): $[\alpha]^{25}_D$ + 86.1 (*c* 0.17, CH_2Cl_2). ^{1}H NMR ($CDCl_3$, 200 MHz): δ_H 2.05 (5H, s, CH_3 D ring and CH_2), 2.42-2.51 (14H, m, CH_3 BODIPY and CH_2), 3.02-3.10 (3H, m, H4 and CH_2), 3.32-3.45 (1H, m, H4), 3.90-4.0 1 (1H, m, H3a), 5.91 (1H, d, *J* = 7.8 Hz, H8b), 6.04 (2H, s, BODIPY), 6.18 (1H, br, H3'), 6.97 (1H, br, H2'), 7.16 (1H, d, *J* = 8.0 Hz, H5), 7.46-7.61 (3H, m, H6, H6' and H8). ^{13}C NMR ($CDCl_3$, 50 MHz): δ_C 10.9 (2 CH_3 BODIPY), 14.6 (2 CH_3 BODIPY), 16.6 (CH_3 D- ring), 27.5 (CH_2*CH*$_2$$CH_2$CONH), 27.6 ($CH_2$*CH*$_2$CONH), 37.0 (*CH*$_2$$CH_2$*CH*$_2$CONH), 37.2 ($CH_2$ C-4a), 39.4 (C-3a), 86.0 (C-8b), 100.7 (C-2'), 113.2 (C-4), 117.7 (C-3'), 121.9 (CH-BODIPY), 122.4 (phenyl *C*-5), 125.7 (C-6'), 131.7 (phenyl, C-3), 136.2 (2C, BODIPY), 137.8 (2C, BODIPY), 138.3 (C, BODIPY), 139.6 (2C, BODIPY), 140.8 (C-4a), 141.1 (phenyl, C-6), 145.5 (C-8a), 151.3 (phenyl, C-8), 154.2 (C-7), 170.4, 171.6 (CONH). EIMS *m*/*z* 323 $[M]^+$ (98), 308 (28), 292 (5), 262 (20), 248 (21), 236 (81), 235 (100), 206 (17), 178 (27), 88 (17). ESI-MS *m*/*z* 652,3 $[M+Na]^+$; HR-ESIMS *m*/*z* 629.2339 (calcd for $C_{34}H_{34}BF_2N_3O_6$: 629,2509).

ent-BPGR24 (12): $[\alpha]^{25}_D$ -82.4 (*c* 0.17, CH_2Cl_2). ^{1}H NMR ($CDCl_3$, 200 MHz): δ_H 2.05 (5H, s, CH_3 D ring and CH_2), 2.42-2.51 (14H, m, CH_3 BODIPY and CH_2), 3.02-3.10 (3H, m, H4 and CH_2), 3.32-3.45 (1H, m, H4), 3.90-4.0 1 (1H, m, H3a), 5.91 (1H, d, *J* = 7.8 Hz, H8b), 6.04 (2H, s, BODIPY), 6.18 (1H, br, H3'), 6.97 (1H, br, H2'), 7.16 (1H, d, *J* = 8.0 Hz, H5), 7.46-7.61 (3H, m, H6, H6' and H8). ^{13}C NMR ($CDCl_3$, 50 MHz): δ_C 10.9 (2 CH_3 BODIPY), 14.6 (2 CH_3 BODIPY), 16.6 (CH_3 D- ring), 27.5 (CH_2*CH*$_2$$CH_2$CONH), 27.6 ($CH_2$*CH*$_2$CONH), 37.0

(*CH*$_2$CH$_2$*CH*$_2$CONH), 37.2 (CH$_2$ C-4a), 39.4 (C-3a), 8BPGR246.0 (C-8b), 100.7 (C-2'), 113.2 (C-4), 117.7 (C-3'), 121.9 (CH-BODIPY), 122.4 (phenyl *C*-5), 125.7 (C-6'), 131.7 (phenyl, C-3), 136.2 (2C, BODIPY), 137.8 (2C, BODIPY), 138.3 (C, BODIPY), 139.6 (2C, BODIPY), 140.8 (C-4a), 141.1 (phenyl, C-6), 145.5 (C-8a), 151.3 (phenyl, C-8), 154.2 (C-7), 170.4, 171.6 (CONH). EIMS *m*/*z* 323 $[M]^+$ (98), 308 (28), 292 (5), 262 (20), 248 (21), 236 (81), 235 (100), 206 (17), 178 (27), 88 (17). ESI-MS *m*/*z* 652,3 $[M+Na]^+$; HR-ESIMS *m*/*z* 629.2339 (calcd for $C_{34}H_{34}BF_2N_3O_6$: 629,2509).

2'-epi-BPGR24 (14): $[\alpha]^{25}_D$ + 148.13 (*c* 0.16, CH_2Cl_2). ^{1}H NMR ($CDCl_3$, 200 MHz): δ_H 2.01 (3H, s, CH_3 D ring), 2.39-2.48 (16H, m, CH_3 BODIPY and 2xCH_2), 2.99-3.07 (3H, m, H4 and CH_2), 3.29-3.42 (1H, m, H4), 3.87-3.98 (1H, m, H3a), 5.88 (1H, d, *J* = 7.8 Hz, H8b), 6.01 (2H, s, BODIPY), 6.14 (1H, br, H3'), 6.94 (1H, br, H2'), 7.13 (1H, d, *J* = 8.0 Hz, H5), 7.43-7.58 (3H, m, H6,H6' and H8). ^{13}C NMR ($CDCl_3$, 50 MHz): δ_C 10.9 (2 CH_3 BODIPY), 14.6 (2 CH_3 BODIPY), 16.6 (CH_3 D-ring), 27.5 (CH_2*CH*$_2$CH$_2$CONH), 27.6 (CH_2*CH*$_2$CONH), 37.1(*CH*$_2$CH$_2$*CH*$_2$CONH), 37.2 (CH_2 C-4a), 39.4 (C-3a), 86.1 (C-8b), 100.9 (C-2'), 113.4 (C-4), 117.7 (C-3'), 122.0 (CH-BODIPY), 122.5 (phenyl *C*-5), 125.8 (C-6'), 131.7 (phenyl, C-3), 136.1 (2C, BODIPY), 137.7 (2C, BODIPY), 138.4 (C, BODIPY), 139.5 (2C, BODIPY), 140.8 (C-4a), 141.2 (phenyl, C-6), 145.5 (C-8a), 151.5 (phenyl, C-8), 154.2 (C-7), 170.4, 171.7 (CONH). EIMS *m*/*z* 323 $[M]^+$ (98), 308 (28), 292 (5), 262 (20), 248 (21), 236 (81), 235 (100), 206 (17), 178 (27), 88 (17); ESI-MS *m*/*z* 652,2 $[M+Na]^+$; HR-ESIMS *m*/*z* 629,2327 (calcd for $C_{34}H_{34}BF_2N_3O_6$: 629,2509).

ent-2'epi-BPGR24 (13): $[\alpha]^{25}_D$ − 175.0 (*c* 0.14, CH_2Cl_2). ^{1}H NMR ($CDCl_3$, 200 MHz): δ_H 2.01 (3H, s, CH_3 D ring), 2.39-2.48 (16H, m, CH_3 BODIPY and 2xCH_2), 2.99-3.07 (3H, m, H4 and CH_2), 3.29-3.42 (1H, m, H4), 3.87-3.98 (1H, m, H3a), 5.88 (1H, d, *J* = 7.8 Hz, H8b), 6.01 (2H, s, BODIPY), 6.14 (1H, br, H3'), 6.94 (1H, br, H2'), 7.13 (1H, d, *J* = 8.0 Hz, H5), 7.43-7.58 (3H, m, H6,H6' and H8). ^{13}C NMR ($CDCl_3$, 50 MHz): δ_C 10.9 (2 CH_3 BODIPY), 14.6 (2 CH_3 BODIPY), 16.6 (CH_3 D-ring), 27.5 (CH_2*CH*$_2$CH$_2$CONH), 27.6 (CH_2*CH*$_2$CONH), 37.1(*CH*$_2$CH$_2$*CH*$_2$CONH), 37.2 (CH_2 C-4a), 39.4 (C-3a), 86.1 (C-8b), 100.9 (C-2'), 113.4 (C-4), 117.7 (C-3'), 122.0 (CH-BODIPY), 122.5 (phenyl *C*-5), 125.8 (C-6'), 131.7 (phenyl, C-3), 136.1 (2C, BODIPY), 137.7 (2C, BODIPY), 138.4 (C, BODIPY), 139.5 (2C, BODIPY), 140.8 (C-4a), 141.2 (phenyl, C-6), 145.5 (C-8a), 151.5 (phenyl, C-8), 154.2 (C-7), 170.4, 171.7 (CONH).

EIMS *m/z* 323 $[M]^+$ (98), 308 (28), 292 (5), 262 (20), 248 (21), 236 (81), 235 (100), 206 (17), 178 (27), 88 (17); ESI-MS *m/z* 652,2 $[M+Na]^+$; HR-ESIMS *m/z* 629,2327 (calcd for $C_{34}H_{34}BF_2N_3O_6$: 629,2509).

X-ray analysis. Crystals that were suitable for X-ray diffraction analyses were obtained via the slow evaporation of a methanol solution. X-ray data were collected on an Oxford Diffraction Gemini R-Ultra diffractometer equipped Enhanced Ultra (Cu) X-ray Source (mirror monochromatized Cu-Kα radiation, λ=1.5418 Å). The ω scan was performed with a frame width of 1.0°. The intensities were corrected for absorption with the numerical correction based on a Gaussian integration over a multifaceted crystal model. Softwares used: CrysAlisPro (Agilent Technologies, Version 1.171.37.31) for data collection, data reduction and absorption correction; SHELXT[40] for data solution; SHELXL-2014/7[40] for refinement; OLEX2 (version 1.2.5)[41] structure analysis and drawing preparation. All non-hydrogen atoms were anisotropically refined. Hydrogen atoms were calculated and refined riding with U_{iso}=1.2 or 1.5 U_{eq} of the atom connected. The absolute configuration was determined using the Parson's method.[27]

ASSOCIATED CONTENT

^{1}H and ^{13}C NMR spectra, CD spectra, $[\alpha]^D$ data, details and CIF file of X-ray data. The Supporting Information is available free of charge on the ACS Publication website at http://pubs.acs.org.

AUTHOR INFORMATION

Corresponding Author

Corresponding Authors *E-mail: cristina.prandi@unito.it. *Tel: (+39) 011 6707647. Notes The authors declare no competing financial interest.

ACKNOWLEDGMENT

We thank the Cost Association STREAM FA1206 "Strigolactones: biological roles and applications", Compagnia di San Paolo Foundation for their support (proJect SLEPS), the

Lagrange ProJect – CRT Foundation/ISI for their grant, and the Italian Ministry of Universities and Research as well as Regione Piemonte.

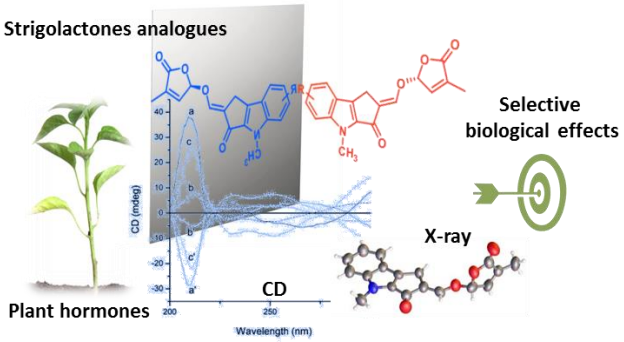

REFERENCES

(1) (a) Zwanenburg, B.; Pospíšil, T. *Mol. Plant* **2013**, *6*, 38-62; (b) Ćavar, S.; Zwanenburg, B.; Tarkowski, P. *Phyt. Rev.* **2014**; (c) Yoneyama, K.; Xie, X.; Yoneyama, K.; Takeuchi, Y. *Pest Manag. Sci.* **2009**, *65*, 467-470.

(2) (a) Gomez-Roldan, V.; Fermas, S.; Brewer, P. B.; Puech-Pagès, V.; Dun, E. A.; Pillot, J. P.; Letisse, F.; Matusova, R.; Danoun, S.; Portais, J. C.; Bouwmeester, H.; Bécard, G.; Beveridge, C. A.; Rameau, C.; Rochange, S. F. *Nature* **2008**, *455*, 189-194; (b) Leyser, O. *Dev. Cell* **2008**, *15*, 337-338; (c) Shinohara, N.; Taylor, C.; Leyser, O. *PLoS Biol.* **2013**, *11*; (d) Rameau, C.; Bertheloot, J.; Leduc, N.; Andrieu, B.; Foucher, F.; Sakr, S. *Front. Plant Sci.* **2015**, *5*.

(3) (a) Koltai, H. *Ann. Bot.* **2013**, *112*, 409-415; (b) Rasmussen, A.; Depuydt, S.; Goormachtig, S.; Geelen, D. *Planta* **2013**, *238*, 615-626; (c) Koltai, H. *New Phytol.* **2011**, *190*, 545-549.

(4) Urquhart, S.; Foo, E.; Reid, J. B. *Physiol. Plantarum* **2015**, *153*, 392-402.

(5) (a) Akiyama, K.; Matsuzaki, K. I.; Hayashi, H. *Nature* **2005**, *435*, 824-827; (b) Ruyter-Spira, C.; Bouwmeester, H. *New Phytol.* **2012**, *195*, 730-733; (c) Bonfante, P.; Genre, A. *Trends Plant Sci.* **2015**, *20*, 150-154.

(6) (a) Akiyama, K.; Hayashi, H. *Ann. Bot.* **2006**, *97*, 925-931; (b) Yoneyama, K.; Xie, X.; Sekimoto, H.; Takeuchi, Y.; Ogasawara, S.; Akiyama, K.; Hayashi, H.; Yoneyama, K. *New Phytol.* **2008**, *179*, 484-494; (c) Zwanenburg, B.; Mwakaboko, A. S.; Reizelman, A.; Anilkumar, G.; Sethumadhavan, D. *Pest Manag. Sci.* **2009**, *65*, 478-491.

(7) (a) Ueno, K.; Furumoto, T.; Umeda, S.; Mizutani, M.; Takikawa, H.; Batchvarova, R.; Sugimoto, Y. *Phytochemistry* **2014**, *108*, 122-128; (b) Nomura, S.; Nakashima, H.; Mizutani, M.; Takikawa, H.; Sugimoto, Y. *Plant Cell Rep.* **2013**, *32*, 829-838.

(8) Yoneyama, K. *J.Pest. Sci.* **2010**, *35*, 348-350.

(9) (a) Pollock, C. B.; McDonough, S.; Wang, V. S.; Lee, H.; Ringer, L.; Li, X.; Prandi, C.; Lee, R. J.; Feldman, A. S.; Koltai, H.; Kapulnik, Y.; Rodriguez, O. C.; Schlegel, R.;

Albanese, C.; Yarden, R. I. *Oncotarget* **2014**, *5*, 1683-1698; (b) Pollock, C. B.; Koltai, H.; Kapulnik, Y.; Prandi, C.; Yarden, R. I. *Breast Cancer Res. Tr.* **2012**, *134*, 1041-1055.

(10) For Michael acceptors natural compounds acting as anticancer agents see Sinisi, A.; Millán, E.; Abay, S. M.; Habluetzel, A.; Appendino, G.; Muñoz, E.; Taglialatela-Scafati, O. J. Nat. Prod. 2015 ASAP and references therein.

(11) (a) Zwanenburg, B.; Nayak, S. K.; Charnikhova, T. V.; Bouwmeester, H. J. *Bioorgan. Med. Chem. Lett.* **2013**, *23*, 5182-5186; (b) Mwakaboko, A. S.; Zwanenburg, B. *Plant Cell Physiol.* **2011**, *52*, 699-715.

(12) Ueno, K.; Sugimoto, Y.; Zwanenburg, B. *Phytochem. Rev.* **2014**, 1-13.

(13) Xie, X.; Yoneyama, K.; Kisugi, T.; Uchida, K.; Ito, S.; Akiyama, K.; Hayashi, H.; Yokota, T.; Nomura, T.; Yoneyama, K. *Mol. Plant* **2013**, *6*, 153-163.

(14) Hamiaux, C.; Drummond, R. S. M.; Janssen, B. J.; Ledger, S. E.; Cooney, J. M.; Newcomb, R. D.; Snowden, K. C. *Curr. Biol.* **2012**, *22*, 2032-2036.

(15) (a) Kagiyama, M.; Hirano, Y.; Mori, T.; Kim, S. Y.; Kyozuka, J.; Seto, Y.; Yamaguchi, S.; Hakoshima, T. *Genes Cells* **2013**, *18*, 147-160; (b) Zhao, J.; Wang, T.; Wang, M.; Liu, Y.; Yuan, S.; Gao, Y.; Yin, L.; Sun, W.; Peng, L.; Zhang, W.; Wan, J.; Li, X. *Plant Cell Physiol.* **2014**, *55*, 1096-1109.

(16) Jiang, L.; Liu, X.; Xiong, G.; Liu, H.; Chen, F.; Wang, L.; Meng, X.; Liu, G.; Yu, H.; Yuan, Y.; Yi, W.; Zhao, L.; Ma, H.; He, Y.; Wu, Z.; Melcher, K.; Qian, Q.; Xu, H. E.; Wang, Y.; Li, J. *Nature* **2013**, *504*, 401-+.

(17) Chiwocha, S. D. S.; Dixon, K. W.; Flematti, G. R.; Ghisalberti, E. L.; Merritt, D. J.; Nelson, D. C.; Riseborough, J. A. M.; Smith, S. M.; Stevens, J. C. *Plant Sci.* **2009**, *177*, 252-256.

(18) Scaffidi, A.; Waters, M. T.; Sun, Y. K.; Skelton, B. W.; Dixon, K. W.; Ghisalberti, E. L.; Flematti, G. R.; Smith, S. M. *Plant Physiol.* **2014**, *165*, 1221-1232.

(19) Umehara, M.; Mengmeng, C.; Akiyama, K.; Akatsu, T.; Seto, Y.; Hanada, A.; Weiqiang, L.; Takeda-Kamiya, N.; Morimoto, Y.; Yamaguchi, S. *Plant Cell Physiol.* **2015**, 1059-1072.

(20) Prandi, C.; Ghigo, G.; Occhiato, E. G.; Scarpi, D.; Begliomini, S.; Lace, B.; Alberto, G.; Artuso, E.; Blangetti, M. *Org. Biomol. Chem.* **2014**, *12*, 2960-2968.

(21) (a) Cohen, M.; Prandi, C.; Occhiato, E. G.; Tabasso, S.; Wininger, S.; Resnick, N.; Steinberger, Y.; Koltai, H.; Kapulnik, Y. *Mol. Plant* **2013**, *6*, 141-152; (b) Prandi, C.; Occhiato, E. G.; Tabasso, S.; Bonfante, P.; Novero, M.; Scarpi, D.; Bova, M. E.; Miletto, I. *Eur. J. Org. Chem.* **2011**, 3781-3793.

(22) Prandi, C.; Rosso, H.; Lace, B.; Occhiato, E. G.; Oppedisano, A.; Tabasso, S.; Alberto, G.; Blangetti, M. *Mol. Plant* **2013**, *6*, 113-127.

(23) Bhattacharya, C.; Bonfante, P.; Deagostino, A.; Kapulnik, Y.; Larini, P.; Occhiato, E. G.; Prandi, C.; Venturello, P. *Org. Biomol. Chem.* **2009**, *7*, 3413-3420.

(24) (a) Pereira, N. A. M.; Pinho e Melo, T. M. V. D. *Org. Prep. Proced. Int.* **2014**, *46*, 183-213; (b) Ni, Y.; Wu, J. *Org. Biomol. Chem.* **2014**, *12*, 3774-3791; (c) Ptaszek, M.: Rational Design of Fluorophores for In Vivo Applications. In *Fluorescence-Based Biosensors: From Concepts to Applications*; Morris, M. C., Ed.; Progress in Molecular Biology and Translational Science, 2013; Vol. 113; pp 59-108.

(25) Reizelman, A.; Wigchert, S. C. M.; Del-Bianco, C.; Zwanenburg, B. *Org. Biomol. Chem.* **2003**, *1*, 950-959.

(26) Kaminski, Z. J.; Paneth, P.; Rudzinski, J. *J. Org. Chem.* **1998**, *63*, 4248-4255.

(27) S. Parsons, H. D. F. a. T. W. *Acta Cryst.* **2013**, 249-259

(28) Crystallographic data for the structure reported in this paper have been deposited with the Cambridge Crystallographic Data Centre with the CCDC number 1403160. Copies of the data can be obtained, free of charge, on application to the Director, CCDC, 12 Union Road, Cambridge CB2 1EZ, UK (fax: +44-(0)1223-336033 or e-mail: deposit@ccdc.cam.ac.uk).

(29) Frischmuth, K.; Wagner, U.; Samson, E.; Weigelt, D.; Koll, P.; Meuer, H.; Sheldrick, W. S.; Welzel, P. *Tetrahedron-Asymmetr.* **1993**, *4*, 351-360.

(30) Nomura, S.; Nakashima, H.; Mizutani, M.; Takikawa, H.; Sugimoto, Y. *Plant Cell Reports* **2013**, *32*, 829-838.

(31) Santoro, E.; Mazzeo, G.; Petrovic, A. G.; Cimmino, A.; Koshoubu, J.; Evidente, A.; Berova, N.; Superchi, S. *Phytochemistry* **2015**, *116*, 359-366.

(32) Scaffidi, A.; Waters, M. T.; Sun, Y. K.; Skelton, B. W.; Dixon, K. W.; Ghisalberti, E. L.; Flematti, G. R.; Smith, S. M. *Plant Physiology* **2014**, *165*, 1221-1232.

(33) Kapulnik, Y.; Delaux, P. M.; Resnick, N.; Mayzlish-Gati, E.; Wininger, S.; Bhattacharya, C.; Séjalon-Delmas, N.; Combier, J. P.; Bécard, G.; Belausov, E.; Beeckman, T.; Dor, E.; Hershenhorn, J.; Koltai, H. *Planta* **2011**, *233*, 209-216.

(34) Cohen, M.; Prandi, C.; Occhiato, E. G.; Tabasso, S.; Wininger, S.; Resnick, N.; Steinberger, Y.; Koltai, H.; Kapulnik, Y. *Mol. Plant* **2013**, *6*, 141-152.

(35) Kretzschmar, T.; Kohlen, W.; Sasse, J.; Borghi, L.; Schlegel, M.; Bachelier, J. B.; Reinhardt, D.; Bours, R.; Bouwmeester, H. J.; Martinoia, E. *Nature* **2012**, *483*, 341-344.

(36) Sasse, J.; Simon, S.; Gübeli, C.; Liu, G. W.; Cheng, X.; Friml, J.; Bouwmeester, H.; Martinoia, E.; Borghi, L. *Curr. Biol.* **2015**, *25*, 647-655.

(37) Fridlender, M. L., B.; Wininger, S,; Dam, A.; Kumari, P.; Belausov, E.; Tsemach, H.; Kapulnik, Y.; Prandi, C.; Koltai, K. *Mol. Plant* **2015**, *in press*, 10.1016/j.molp.2015.1008.1013.

(38) Umpublished data

(39) Zwanenburg, B.; Thuring, J. *Pure and Applied Chemistry* **1997**, *69*, 651-654.

(40) Sheldrick, S. M. *Acta Cryst.* **2015**, *A71*, 3-8.

(41) O. V. Dolomanov, L. J. B., R. J. Gildea, J. A. K. Howard and H. Puschmann. *Appl. Cryst.* **2009**.